

# A COMPARATIVE STUDY OF SINGLE-SWITCH, THREE-PHASE, HIGH-POWER-FACTOR RECTIFIERS

Yungtaek Jang and Milan M. Jovanović

DELTA Power Electronics Lab., Inc.  
1872 Pratt Drive, Suite 1400  
Blacksburg, VA 24060

**Abstract** - Three three-phase, single-switch, high-power-factor rectifier implementations were evaluated on a comparative basis. Specifically, the discontinuous-conduction-mode boost rectifier with a 5<sup>th</sup>-harmonic-trap filter, the discontinuous-conduction-mode boost rectifier with a harmonic-injection circuit, and the multi-resonant, zero-current-switching buck rectifier were compared with respect to their efficiencies, compliance with the IEC555-2 specifications, volumes, weights, and costs. The comparisons were done for the three-phase, line-to-line input voltage of  $380 V_{\text{rms}} \pm 20\%$  and for 0 - 6 kW output-power range.

## I. Introduction

Low-harmonic, high-power-factor (HPF) rectification in three-phase power systems can be implemented with a large number of topologies and control strategies [1]. Based on the number of controllable switches, HPF rectifiers can be classified as multi- or single-switch rectifiers. Generally, the rectification performance of the multi-switch rectifiers is superior to that of the single-switch rectifiers since the multiple-switch rectifiers can achieve higher power factors and lower harmonic distortions of the line currents. Specifically, six-switch rectifiers have been extensively used in a variety of HPF applications [1].

While the use of multi-switch rectifiers is quite justified in high-power, high-performance applications, the increased number of switches and the complexity of their control make multi-switch rectifiers too expensive in lower power, cost-sensitive applications. For example, today's HPF telecommunication rectifiers, which only need to reduce the total harmonic distortion (THD) of the line current to below 10-15%, are exclusively implemented either with passive LC filters or active, single-switch rectifiers.

So far, several three-phase, HPF rectifiers employing a single switch have been introduced [2]-[4]. Since these rectifiers have a single active switch and perform HPF rectification naturally without a need for a complex control circuitry, they are very suitable for the low-cost, low-power, three-phase ac-dc applications.

In this paper, three single-switch HPF rectifiers were studied and evaluated on a comparative basis. The comparisons were done with respect to their efficiencies,

compliance with the IEC555-2 specifications, volumes, weights, and costs. The rectifiers were designed for the three-phase, line-to-line input voltage of  $380 V_{\text{rms}} \pm 20\%$  and for 0 - 6 kW output-power range. The three topologies compared in this paper are:

- the single-switch, three-phase, discontinuous-conduction-mode (DCM) boost rectifier with a 5<sup>th</sup>-harmonic-trap filter;
- the single-switch, three-phase, DCM boost rectifier with a harmonic-injection circuit; and
- the single-switch, three-phase, multi-resonant, zero-current-switching (ZCS) buck rectifier.

## II. Single-Switch, Three-Phase, DCM Boost Rectifier

The circuit diagram of the power stage of the single-switch, three-phase, PWM, DCM boost rectifier is shown in Fig. 1(a). Since the boost rectifier in Fig. 1(a) is operated in DCM with a constant frequency and constant duty cycle, all three-phase input currents,  $i_a$ ,  $i_b$ , and  $i_c$ , are zero at the end of a switching period, immediately before boost switch S is turned on. After switch S is turned on,  $i_a$ ,  $i_b$ , and  $i_c$  increase linearly to the peak values, which are proportional to the line-to-neutral voltages as shown in Fig. 1(b). Therefore, during the switch-on period, each line current forms a triangular pulse with the peak value proportional to the associated line-to-neutral voltage. As a result, during the switch-on period, the average line currents are proportional to the line-to-neutral voltages. When the switch is turned off, the input currents start decreasing because output voltage  $V_O$  is higher than the peak of the input voltage. In DCM, the input currents reach zero before the end of the switching period. Since the rate of the input-current decrease is proportional to the difference between output voltage  $V_O$  and line-to-neutral voltage, the average line currents during the off period of the switch are not proportional to the line voltages, *i.e.*, even if the line voltages are perfectly balanced and sinusoidal, the line currents are distorted. Figure 2 shows the normalized harmonic content of the rectifier input current as a function of the voltage-conversion ratio  $M$ , which is defined as

$$M = \frac{V_O}{\sqrt{3}V_m} \quad (1)$$

where  $V_O$  is the rectifier output voltage and  $V_m$  is the peak line-to-neutral voltage. As can be seen from Fig. 2, the

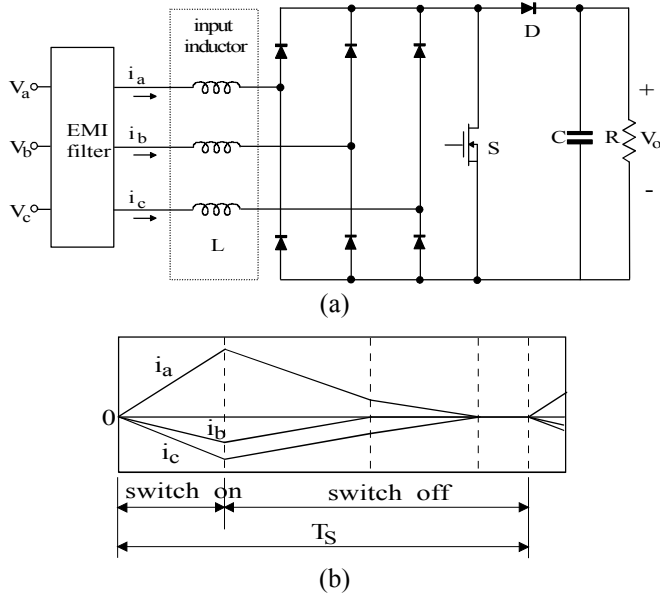


Fig. 1 Single-switch, three-phase DCM boost rectifier: (a) circuit diagram; (b) input current waveforms during switching cycle.

rectifier input-current spectrum, which contains only odd harmonics, is dominated by the 5<sup>th</sup>-order harmonic, *i.e.*, the lowest order harmonic. For example, at  $M = 1.2$ , the 5<sup>th</sup>-order harmonic is 8 times larger than the 7<sup>th</sup>-order harmonic, which is the next largest. Also, it should be noted that the value of the normalized 5<sup>th</sup>-order harmonic monotonically decreases as the value of  $M$  increases. In fact, it decreases from slightly over 30% of the fundamental component at  $M = 1.1$  to approximately 7% at  $M = 2$ .

Generally, the maximum input power at which the three-phase, constant-frequency, DCM boost rectifier can meet the IEC555-2 specifications is limited by the 5<sup>th</sup>-order harmonic of the input current. As an illustration, Fig. 3 shows the 5<sup>th</sup>,

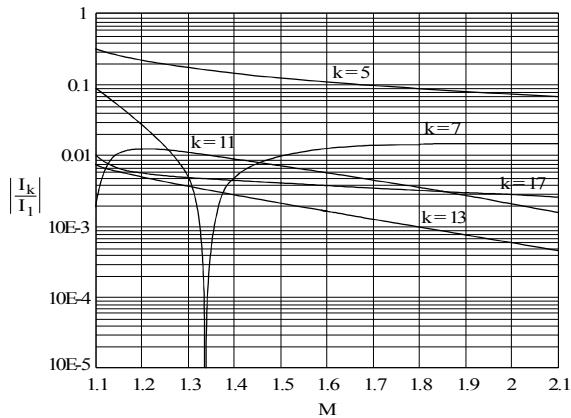


Fig. 2 Normalized input-current harmonics of the single-switch, three-phase, constant-frequency, constant-duty-cycle, DCM boost rectifier. Harmonics are normalized with respect to the fundamental component.

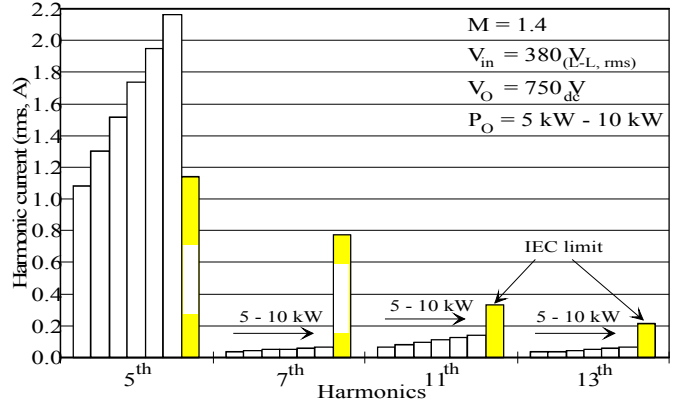


Fig. 3 Comparison between the input-current harmonic content of the single-switch, three-phase, constant-frequency, constant-duty-cycle, DCM boost rectifier and harmonic-current limits of the IEC555-2 for  $M = 1.4$ ,  $V_O = 750$  V,  $V_{in(L-L)} = 380$  V<sub>rms</sub>,  $P_{in} = 5$  kW - 10 kW.

7<sup>th</sup>, 11<sup>th</sup>, and 13<sup>th</sup> harmonics of the DCM boost rectifier with  $M = 1.4$  and input power levels from 5 kW to 10 kW along with the corresponding IEC555-2 limits. As can be seen from Fig. 3, for  $M = 1.4$  the rectifier can meet the IEC555-2 requirements only for power levels up to 5 kW because of the 5<sup>th</sup>-harmonic limitation. The higher-order harmonics, *i.e.*, 7<sup>th</sup>, 11<sup>th</sup>, 13<sup>th</sup>, etc., are well below the IEC555-2 limits, even for power levels over 10 kW.

To meet the IEC555-2 specifications at power levels above 5 kW, the three-phase, constant-frequency, constant-duty-cycle DCM boost rectifier needs to be designed with a higher  $M$ . However, it should be noted that for a given power line voltage, larger  $M$  requires a boost switch with a higher voltage rating, which has a detrimental effect on the conversion efficiency and cost. Nevertheless, the IEC555-2 limits can be met with a relatively low value of  $M$  if either a passive 5<sup>th</sup>-order harmonic-trap filter is used, or the duty-cycle of the switch is modulated by a harmonic-injection signal to attenuate the 5<sup>th</sup>-order harmonic.

### III. DCM Boost Rectifier with 5<sup>th</sup>-Order Harmonic Trap

To reduce the magnitude of the 5<sup>th</sup> harmonic in the input current, the 5<sup>th</sup>-order harmonic-trap filter, which consists of inductances  $L_{T1}$  and  $L_{T2}$  and capacitance  $C_{T2}$ , needs to be added at the input of the power stage, as shown in Fig. 4. If the resonant frequency of the series resonant tank  $L_{T2} - C_{T2}$  is selected at the frequency of the 5<sup>th</sup> harmonic of the line, the 5<sup>th</sup> harmonic of the rectifier current will be mainly flowing through the  $L_{T2} - C_{T2}$  branches of the filter and not through the source. The harmonic-trap inductance  $L_{T1}$  can also be utilized as a part of the differential-mode input filter formed by the addition of filter capacitor  $C_{T1}$ .

Figure 5 shows the harmonic-trap filter and its magnitude frequency response. This filter has a passband between dc and

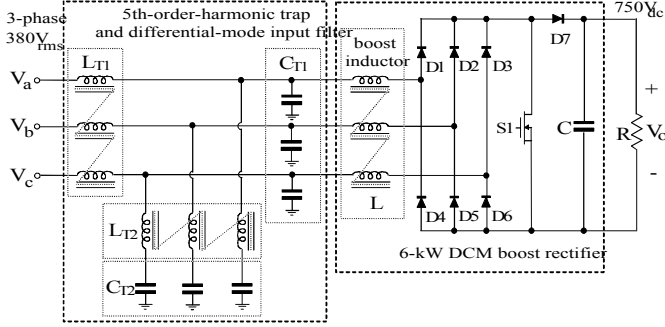


Fig. 4 Single-switch, three-phase DCM boost rectifier with 5<sup>th</sup>-harmonic trap.

cut-off frequency  $f_c$  and provides a steep rate of attenuation from  $f_c$  to notch frequency  $f_\infty$ . The characteristics of the filter in Fig. 5 are completely described by the following design equations [5]:

$$m = \sqrt{1 - \frac{f_c^2}{f_\infty^2}}, \quad L_{T1} = mL_k, \quad L_{T2} = \frac{1 - m^2}{m} L_k,$$

$$C_{T2} = mC_k, \quad f_c = \frac{1}{2\pi\sqrt{L_k C_k}}, \quad \text{and} \quad f_\infty = \frac{1}{2\pi\sqrt{L_{T2} C_{T2}}}.$$

The ratio  $m$  represents the slope of the magnitude characteristic from  $f_c$  to  $f_\infty$ . If the value of  $m$  is unity, then  $L_{T2}$  becomes zero, and  $L_{T1}$  and  $C_{T2}$  are equal to  $L_k$  and  $C_k$  respectively. Therefore, this circuit becomes a simple L-C lowpass filter where  $L_k$  and  $C_k$  are the filter elements which define the cut-off frequency  $f_c$ . As  $m$  in the filter in Fig. 5 decreases, the filter attenuation rate increases. The filter has the flattest impedance over the greatest part of the passband when  $m$  is designed as approximately 0.6. However, the value of  $m$  should be selected so that it results in a good compromise between the attenuation performance and volume and cost.

One problem in using a harmonic trap in a harmonic generating power system (e.g., DCM boost rectifier) is the possibility to excite harmonic resonances [6]. Both series and parallel resonances may occur in a power system due to the existence of the filter and power line reactive components. To further explain these resonances, Fig. 6 shows the equivalent harmonic circuit for a power system that consists of the rectifier bridge and the harmonic trap. In Fig. 6, the DCM boost rectifier is modeled as a harmonic current source. The

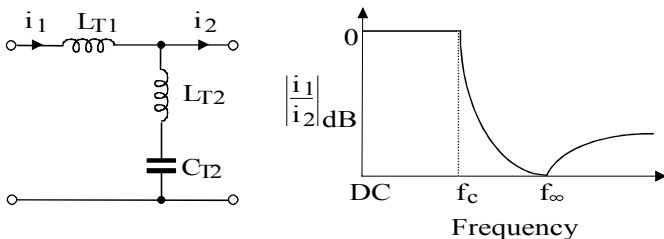


Fig. 5 Harmonic-trap circuit and its frequency response.

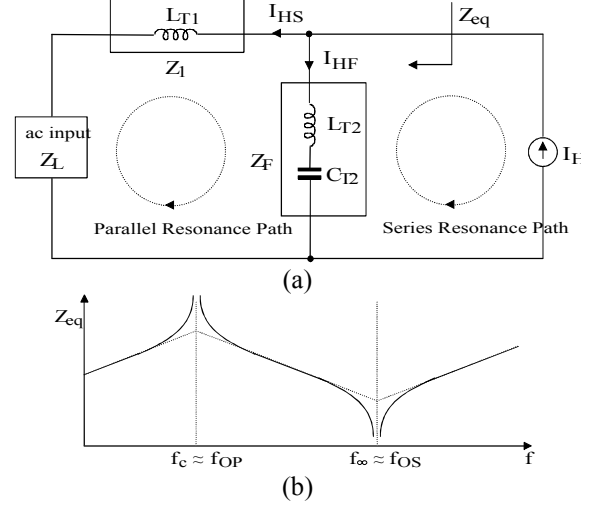


Fig. 6 Harmonic resonances of harmonic-trap filter: (a) equivalent circuit of DCM boost rectifier with harmonic-trap circuit. (b) magnitude vs. frequency plot of output impedance of the filter.

impedances  $Z_F$  and  $Z_1$ , and  $Z_L$  are the filter impedances and the line impedance, respectively. The harmonic current flowing through the trap filter is

$$I_{HF} = I_H \frac{Z_1 + Z_L}{Z_1 + Z_L + Z_F} = I_H \frac{Z_S}{Z_S + Z_F}, \quad (2)$$

while the harmonic current flowing through the source is

$$I_{HS} = I_H \frac{Z_F}{Z_1 + Z_L + Z_F} = I_S \frac{Z_F}{Z_S + Z_F}, \quad (3)$$

where  $Z_S = Z_1 + Z_L$ .

Since at series resonant frequency  $f_{OS} = f_\infty$ ,  $|Z_F| \ll |Z_S|$ , most of the harmonic current flows through the harmonic trap impedance  $Z_F$ . However, at parallel resonant frequency  $f_{OP}$ ,  $|Z_F| = |Z_S|$ , and a high circulating current flows in the loop consisting of the trap filter and the ac source. Therefore, to avoid this problem, the cut-off frequency of the trap filter should always be below the 5<sup>th</sup>-harmonic line frequency, including possible frequency variations.

For 60 Hz line frequency, the 5<sup>th</sup>-harmonic trap filter should have a notch frequency  $f_\infty$  of 300 Hz. To ensure that the cut-off frequency of the filter is safely below 300 Hz, cut-off frequency  $f_c$  should be selected to be  $f_\infty - 10\%$ , or approximately 275 Hz. With this selection of the filter, the parameters and the components values of the filter are  $m = 0.36$ ,  $L_k = 5.9$  mH,  $C_k = 55$  uF,  $L_{T1} = 2.2$  mH,  $L_{T2} = 14.1$  mH, and  $C_{T2} = 20$  uF.

#### IV. DCM Boost Rectifier with Harmonic-Injection Circuit

The harmonic-injection approach does not increase the voltage stress of the boost switch and requires only a few additional components for its implementation [7] - [10]. In the technique presented in [10], a voltage signal which is

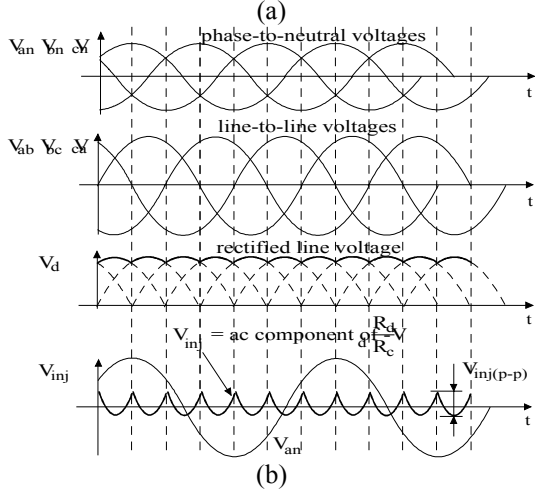
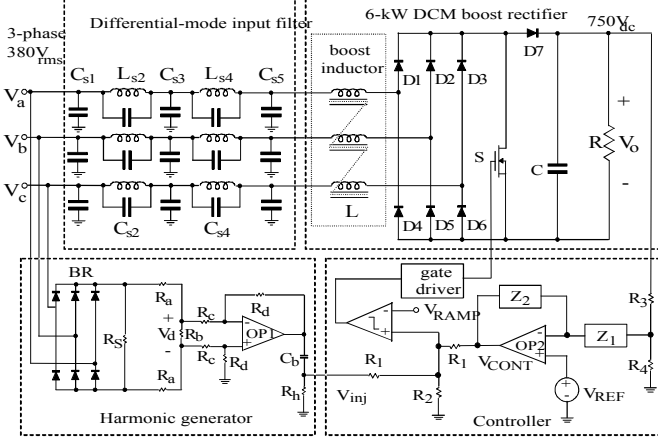


Fig. 7 Single-switch, three-phase DCM boost rectifier with harmonic injection circuit: (a) circuit diagram; (b) key voltage waveforms.

proportional to the inverted ac component of the rectified, three-phase, line-to-line input voltage is injected into the output-voltage feedback loop to vary the duty cycle of the rectifier within a line cycle in order to reduce the 5<sup>th</sup>-order harmonic and improve the THD of the rectifier input currents.

The simplest implementation of the harmonic injection circuit and its key waveforms are shown in Fig. 7 [10]. In the implementation in Fig. 7(a), the three-phase line voltage is first rectified by three-phase bridge rectifier BR, and then attenuated by the resistive voltage divider  $R_a - R_b$ . The scaled-down line voltage developed across  $R_b$ ,  $V_d$ , is then inverted by difference amplifier OP1 before it is processed through the high-pass filter  $C_b - R_h$  to remove the dc component of  $V_d$  and generate injection signal  $V_{inj}$ . Finally,  $V_{inj}$  is injected in the control circuit at the noninverting input of the PWM comparator through summing resistor  $R_1$ .

When signal  $V_{inj}$ , shown in Fig. 7(b), is injected at the PWM modulator, it modifies the duty cycle so that the 5<sup>th</sup>-order harmonic of the input current is reduced and the THD is improved. In fact, since the variation of duty cycle  $d(t)$  is

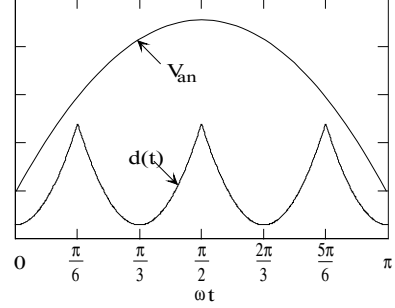


Fig. 8 Duty-cycle variations during half of fundamental line period.

directly proportional to signal  $V_{inj}$ , the modulation of the duty ratio during a line cycle can be described as

$$D_{MOD}(t) = D[1 + d(t)], \quad (4)$$

where  $D_{MOD}$  is the modulated duty cycle,  $D$  is the duty cycle in the absence of the modulation, and  $d(t)$  is the duty cycle modulation. Since  $d(t)$  is proportional to the inverted ac component of the rectified three-phase line-to-line input voltage, the variation of duty cycle  $d(t)$  during half of the fundamental line period can be plotted along with the line-to-neutral input voltage, as shown in Fig. 8.

The periodic function  $d(t)$  in Fig. 8 can be expressed in terms of the Fourier series representation as

$$d(t) = \frac{m}{\pi} \sum_{n=1}^{\infty} \frac{(-1)^n 6}{(6n)^2 - 1} \cos(6n\omega t). \quad (5)$$

From Eq. (5), it can be seen that the generated injection signal contains not only the 6<sup>th</sup>-order harmonic but also higher-order harmonics such as 12<sup>th</sup>, 18<sup>th</sup>, etc. As shown in [10], these higher-order harmonics help to improve the THD more than if only the 6<sup>th</sup>-order harmonic is injected.

At any given voltage-conversion ratio  $M$ , the optimal modulation index  $m$  which produces the minimum THD can be determined. To maximize the input power of the rectifier at which the IEC555-2 specifications are met, modulation index  $m$  should be determined so that the ratio of the 7<sup>th</sup>-order harmonic and the 5<sup>th</sup>-order harmonic is equal to corresponding IEC555-2 limits [10].

## V. Single-Switch, Three-Phase, Multi-Resonant, ZCS Buck Rectifier

Figure 9 shows the three-phase, multi-resonant, ZCS buck rectifier and the voltage waveform across input-side resonant capacitor  $C_{r1}$ . Since input-filter inductors  $L_a, L_b, L_c$ , and output-filter inductor  $L_f$  are relatively large, they have small switching-frequency current ripples. In a steady state, the average voltages of  $C_{r1}-C_{r3}$  during a switching period are equal to the associated input voltages. Because the peak voltages of  $C_{r1}-C_{r3}$  are proportional to the input currents, and switching frequency  $f_s$  is much higher than line frequency  $f_L$ , the input-current waveforms follow the input-voltage waveforms. As a result, the circuit possesses a high power factor and a low harmonic content in the input current.

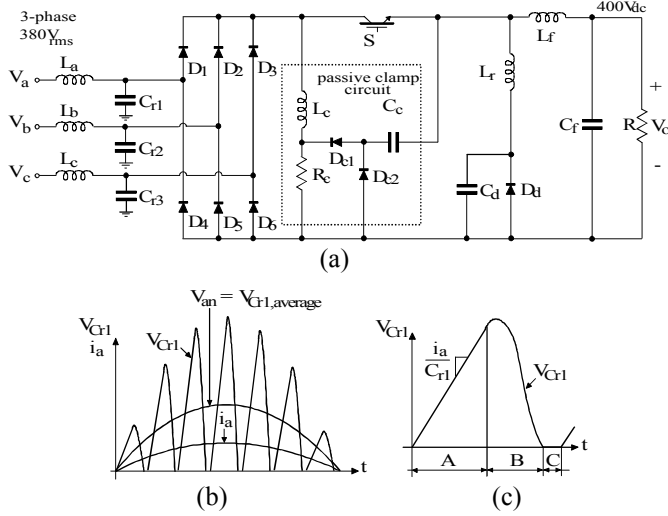


Fig. 9 Multi-resonant, ZCS buck rectifier: (a) circuit diagram, (b) voltage waveform of  $C_{r1}$  and input current waveform  $i_a$ , and (c) enlarged  $V_{Cr1}$  waveform during one switching period.

In the circuit shown in Fig. 9, the amount of input-current distortion depends on the shape of the voltage waveform across  $C_{r1}$ , shown in Fig. 9(c). During the first period, when

switch  $S$  is off,  $V_{Cr1}$  is increasing linearly with a slope proportional to input current  $i_a$ . During the second period when switch  $S$  is on, resonant capacitor  $C_{r1}$  resonates with inductor  $L_r$ , until  $V_{Cr1}$  reaches zero voltage. Finally,  $V_{Cr1}$  remains at zero for the third period, during which switch  $S$  is still on. Since  $V_{Cr1}$  is proportional to input current  $i_a$  only during the off time of switch  $S$ , the input-current waveform becomes more proportional to the input-voltage waveform if the first period is longer than the sum of the second and the third periods. Because in the multi-resonant scheme in Fig. 9 the durations of the second and third periods are significantly reduced, the circuit performs the rectification with a low THD.

## VI. Evaluation Results

To compare the performance of the three rectifier topologies, the three circuits were built for the three-phase, line-to-line input voltage of  $380 V_{rms} \pm 20\%$  and for 0 - 6 kW output-power range. The power-stage and input-filter components used in the three experimental prototypes are given in Table 1.

The output voltage of the DCM boost rectifiers with the 5<sup>th</sup>-order harmonic trap and the harmonic injection was 750 V, whereas the output voltage of the ZCS buck rectifier

Table 1 Components of rectifiers

Rectifiers	DCM boost rectifier with 5 <sup>th</sup> -harmonic trap filter	DCM boost rectifier with harmonic-injection circuit	Multi-resonant, ZCS buck rectifier
<b>Power Stage Components</b>			
Switch S	APT10026 (1000 V, 33 A)	APT10026 (1000 V, 33 A)	2 × IXSH35N140A (1400 V, 35 A) in Parallel
Input Bridge Diode $D_{in}$	BYT230PIV-1000 (1000 V, 30 A)	BYT230PIV-1000 (1000 V, 30 A)	2 × DSEI30-10A (1000 V, 30 A) in series
Output Diode D	DSEI60-10A (1000 V, 60 A)	DSEI60-10A (1000 V, 60 A)	2 × DSEI30-10A (1000 V, 30 A) in series
Boost Inductor	$L = 3 \times 42 \mu\text{H}$	$L = 3 \times 42 \mu\text{H}$	None
<b>Input Filter Components</b>			
Inductors	$L_{T1} = 3 \times 2.2 \text{ mH}$ , $L_{T2} = 3 \times 14 \text{ mH}$	$L_{S2} = 3 \times 140 \mu\text{H}$ , $L_{S4} = 3 \times 160 \mu\text{H}$	$L_a - L_c = 0.9 \text{ mH}$
Capacitors	$C_{T1} = 3 \times 1 \mu\text{F}$ $C_{T2} = 3 \times 20 \mu\text{F}$	$C_{S1} = 3 \times 2.7 \mu\text{F}$ , $C_{S2} = 3 \times 47 \text{ nF}$ $C_{S3} = 3 \times 6.8 \mu\text{F}$ , $C_{S4} = 3 \times 0.1 \mu\text{F}$ $C_{S5} = 3 \times 5.6 \mu\text{F}$	None
<b>Output Filter Components</b>			
Inductors	None	None	$L_f = 0.8 \text{ mH}$
Capacitors	$C = 330 \mu\text{F}$	$C = 330 \mu\text{F}$	$C_f = 470 \mu\text{F}$
<b>Resonant Components</b>			
Inductors	None	None	$L_r = 43 \mu\text{H}$
Capacitors	None	None	$C_{r1} - C_{r3} = 133 \text{ nF}$ , $C_d = 80 \text{ nF}$

**Table 2 Comparisons of volumes, weights, and costs of rectifiers**

Rectifiers	Inductive Components	Capacitive Components	Control Circuit	Power Stage	Overall Volume	Overall Weight	Cost
<b>DCM boost rectifier with 5<sup>th</sup>-harmonic trap filter</b>	3000 cm <sup>3</sup>	2000 cm <sup>3</sup>	1000 cm <sup>3</sup>	2000 cm <sup>3</sup>	8000 cm <sup>3</sup>	10.5 kg	Medium
<b>DCM boost rectifier with harmonic injection</b>	1000 cm <sup>3</sup>	1000 cm <sup>3</sup>	1000 cm <sup>3</sup>	2000 cm <sup>3</sup>	5000 cm <sup>3</sup>	5 kg	Low
<b>Multi-resonant, ZCS buck rectifier</b>	1700 cm <sup>3</sup>	1000 cm <sup>3</sup>	1000 cm <sup>3</sup>	2300 cm <sup>3</sup>	6000 cm <sup>3</sup>	6.4 kg	High

was 400 V. The output voltages of the boost prototype circuits were controlled with a constant-frequency PWM control at 45 kHz. Due to the wide input-voltage and load ranges, the closed-loop control of the buck prototype rectifier was implemented by a combination of a variable- and constant-frequency control. The circuit is controlled by the frequency control for the output power in the range from 6 kW to 600 W. In this power range, the switching frequency of the rectifier varies from 90 kHz at full power to 20 kHz at 10% load. When the output power falls below 600 W at the nominal input voltage, the constant frequency PWM control takes over [11]. Since with a constant-frequency PWM control, the switch operates with “hard” switching, the passive clamp circuit is used to limit the maximum voltage of the switch. Because in the constant-frequency PWM control mode the output power is low, the clamping circuit operates with negligible losses.

Table 2 summarizes the overall volumes and weights of the three prototypes. In addition, Table 2 also shows the volumes of inductive and capacitive components separately, as well as the volumes of the control circuits and power stages. Similarly, Figs. 10 to 12 show the comparisons between the measured input-current harmonic content of the experimental rectifiers and the IEC555-2 harmonic-current limits at different input voltages. Finally, Fig. 13 presents the measured efficiencies of the experimental prototypes.

As can be seen from the presented experimental data, the 5<sup>th</sup>-harmonic trap reduces the 5<sup>th</sup>-order harmonic in the input current so that the rectifier produces THD from 6% to 11%, and achieves 95.8% to 97.6% efficiency at the full load and output voltage  $V_o = 750 V_{dc}$ . The THD and all harmonic currents meet the IEC555-2 requirements over the entire input-voltage and output-power ranges. However, as shown in Table 2, the size and, especially, the weight of the circuit with the 5<sup>th</sup>-harmonic trap is significantly greater than the size and weight of the other topologies. The approximate overall volume and weight are 8000 cm<sup>3</sup> and 10.5 kg, respectively.

The DCM boost-rectifier with the harmonic-injection circuit has THD from 7.5% to 12.9% and efficiency from 96.4% to 98% at the full load and for  $V_o = 750 V_{dc}$ . The approximate overall volume and weight are 5000 cm<sup>3</sup> and 5 kg, respectively.

Finally, the multi-resonant ZCS buck rectifier can achieve the THD less than 5% over the input-voltage and output-power ranges. Efficiency of the rectifier is about 95% at the full load and for  $V_o = 400 V$ . The approximate overall volume and weight are 6000 cm<sup>3</sup> and 6.4 kg, respectively. Although the multi-resonant, buck-type rectifier exhibits the lowest THD, the stresses on the semiconductor devices, together with their conduction losses, result in its limited efficiency and higher cost.

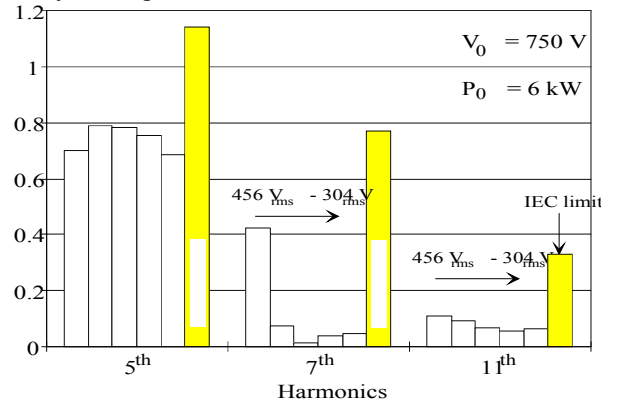


Fig. 10 Comparison of input-current harmonic content of experimental 6-kW DCM boost rectifier with 5<sup>th</sup>-harmonic trap and IEC555-2 harmonic-current limits at different input voltages.

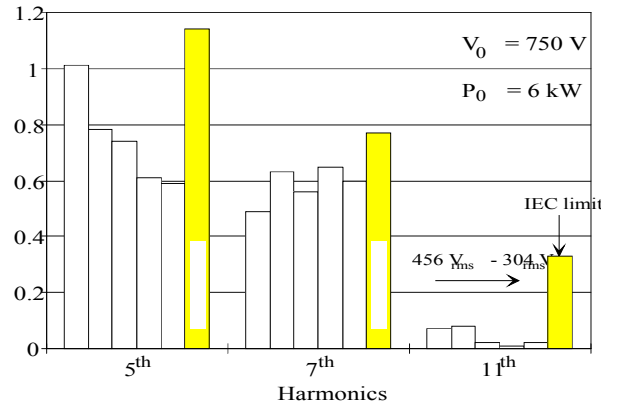


Fig. 11 Comparison of input-current harmonic content of experimental 6-kW DCM boost rectifier with harmonic injection circuit and IEC555-2 harmonic-current limits at different input voltages.

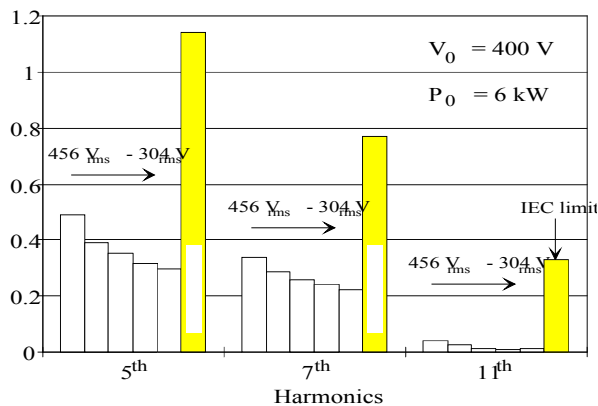


Fig. 12 Comparison of input-current harmonic content of experimental 6-kW multi-resonant, ZCS buck rectifier and IEC555-2 harmonic-current limits at different input voltages.

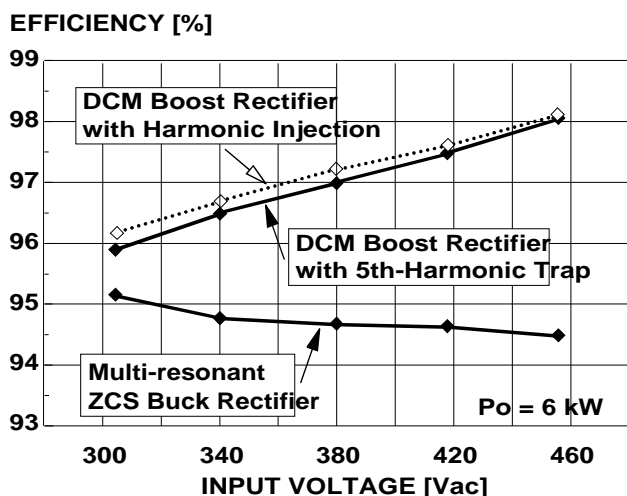


Fig. 13 Measured efficiency of experimental prototypes.

## VII. Summary

The performance comparisons of the three-phase, DCM boost rectifiers with the 5<sup>th</sup>-harmonic trap filter and the harmonic-injection control, and the multi-resonant, zero-current-switching buck rectifier show that the DCM boost rectifier with harmonic-injection control can be implemented to meet the IEC555-2 specification with the smallest size and weight, as well as the highest efficiency. However, if total-harmonic distortion below 5% is required, the single-switch, multi-resonant, ZCS buck rectifier appears to be the only viable approach.

## References

- [1] F.C. Lee, D. Boroyevich, "Power Factor Correction Circuits Topologies and Control," *IEEE Applied Power Electronics Conference (APEC) Professional Education Seminars Workbook*, Seminar 4, 1993.
- [2] A.R. Prasad, P.D. Ziogas, S. Manias, "An Active Power Factor Correction Technique for Three-Phase Diode Rectifiers," *IEEE Power Electronics Specialists Conf. (PESC) Record*, 1989, pp. 58 - 66.
- [3] E.H. Ismail, R.W. Erickson, "A Single Transistor Three Phase Resonant Switch for High Quality Rectification," *IEEE Power Electronics Specialists Conf. (PESC) Record*, 1992, pp. 1341 - 1351.
- [4] Y. Jang, R.W. Erickson, "New Single-Switch Three-Phase High Power Factor Rectifiers Using Multi-Resonant Zero Current Switching," *IEEE Applied Power Electronics Conference (APEC) Proc.*, 1994, pp. 711 - 717.
- [5] J.W. Clark, *AC Power Conditioners*, Academic Press, San Diego, 1990.
- [6] E. H. Ismail, "Three-Phase High Quality Rectification," Ph. D. Thesis, University of Colorado, Boulder, 1993.
- [7] J. W. Kolar, H. Ertl, F. C. Zach, "Space Vector-Based Analytical Analysis of the Input Current Distortion of A Three-Phase Discontinuous-Mode Boost Rectifier System," *IEEE Power Electronics Specialists Conf. (PESC) Record*, 1993, pp. 696 - 703.
- [8] Q. Huang, F.C. Lee, "Harmonic Reduction in A Single-Switch, Three-Phase Boost Rectifier with High Order Harmonic Injected PWM," *IEEE Power Electronics Specialists Conf. (PESC) Record*, 1996, pp. 1266 - 1271.
- [9] J. Sun, N. Frohliche, H. Grotstollen, "Harmonic Reduction Techniques for Single-Switch Three-Phase Boost Rectifiers," *IEEE IAS Annual Meeting Record*, 1996, pp. 1225 - 1232.
- [10] Y. Jang, M.M. Jovanovi}, "A Novel, Robust, Harmonic Injection Method for Single-Switch, Three-Phase, Discontinuous-Conduction-Mode Boost Rectifiers," *IEEE Power Electronics Specialists Conf. (PESC) Record*, 1997, pp. 469 - 475.
- [11] Y. Jang, M.M. Jovanovi}, "Design Considerations and Performance Evaluation of A 6-kW, Single-Switch, Three-Phase, High-Power-Factor, Multi-Resonant, Zero-Current-Switching Buck Rectifier," *IEEE Int'l Telecommunications Energy Conf. Proc.*, 1997, pp. 715 - 722.